POLSKA AKADEMIA NAUK
Instytut Badań Systemowych

ESSAYS ON STABILITY ANALYSIS AND MODEL REDUCTION

Umberto Viaro

Warsaw 2010

SYSTEMS RESEARCH INSTITUTE
POLISH ACADEMY OF SCIENCES
Series: SYSTEMS RESEARCH
Volume 68

Series Editor:

Prof. Jakub Gutenbaum

Warsaw 2010

SYSTEMS RESEARCH INSTITUTE
POLISH ACADEMY OF SCIENCES

==========

Umberto Viaro

ESSAYS ON STABILITY ANALYSIS AND MODEL REDUCTION

Warsaw 2010

Prof. Umberto Viaro
Dipartimento di Ingegneria Elettrica, Gestionale e Meccanica
Università degli Studi di Udine
via delle Scienze 208, 33100 Udine, Italy
email: viaro@uniud.it

Preface by Prof. Wiesław Krajewski
Systems Research Institute
Polish Academy of Sciences
01-447 Warsaw, Newelska 6
Wieslaw.Krajewski@ibspan.waw.pl

Papers Reviewers:

Prof. Jerzy Klamka
Prof. Stanisław Bańka

Partially supported by the University of Udine

ISSN 0208-8029

ISBN 9788389475282

Chapter 9

Feedback control in ancient clocks

Even if the word "feedback" was coined in the early 90s (very likely, it was first used in the journal *Wireless* devoted to electronics and telecommunications in 1923), the feedback principle has been exploited, often in an unconscious way, since the dawn of technology [1]. It is not surprising that the earliest feedback device on record is a timepiece, the ingenious water clock of Ktesibios which dates back to the first half of the third century B.C. [2]. On the other hand, in his celebrated book *The Origins of Feedback Control* [3], Otto Mayr does not mention any mechanical clockwork as an example of closed–loop control in the history of technology. However, many medieval clocks do exert feedback control to produce precisely regulated motion by means of a mechanism called "escapement" [4]. In particular, the feedback nature of the weight–driven *verge–and–foliot* escapement has been pointed out in [5]. This escapement was the only mechanical escapement known from the time of its inception (the first mention of these clocks in a literary context can be found in Dante's *Divine Comedy* [6]) until the middle of the 17th century [7]: in 1657 Huygens modified the verge–and–foliot escapement by replacing the foliot (a bar swinging in a horizontal plane) with a pendulum oscillating in a vertical plane and the crown gear mounted horizontally [8].

This chapter analyzes the operation of the verge–and–foliot escapement along the lines of [5] which have been further developed in [7]. Precisely, Section 9.1 describes the escapement mechanism which consists of a pair of rotating rigid bodies interacting through collisions. Section 9.2 derives the motion equations of the escapement under the assumptions of inelastic collisions. The block diagram describing the system operation is shown in Section 9.3 where the crown–gear angular velocity is determined. The case of elastic collisions in considered in Section 9.4. Some concluding remarks are drawn in Section 9.5. The interested reader is referred to [7] for a detailed analysis of the system operation corresponding to arbitrary values of the coefficient of restitution.

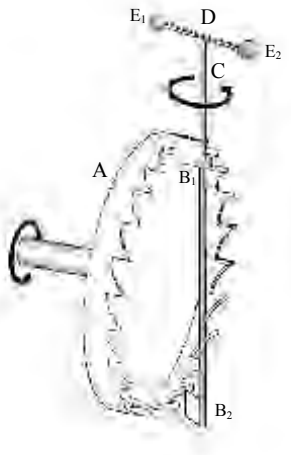

Figure 9.1: Outline of the verge–and–foliot escapement.

9.1 Verge–and–foliot escapement

In the medieval mechanical clocks, the motive power was supplied by falling weights, as in the recent grandfather clocks. The crucial problem was to control this movement so as to ensure a regular velocity of the indicating element (the hand). This result was obtained by means of the so–called verge–and–foliot escapement which consists of two rigid bodies rotating on bearings. Such a device is sketched in Fig. 9.1.

A crown gear A with an odd number of saw–like teeth, being driven

round by the pull of a weight, alternately hits the two blades B_1 and B_2 (the so–called pallets) fastened to a shaft C (the so–called verge). This shaft is connected with a bar D (the so–called foliot) with adjustable weights on its ends (E_1 and E_2). The revolving motion of the crown gear causes an alternating circular movement of the foliot: a push on the upper blade B_1 gives rise to a rotary movement in one direction (e.g., clockwise) whereas a push on the lower blade B_2 gives rise to a rotary movement in the opposite direction (e.g., counterclockwise). This is presumably the reason why the foliot has been given such a name: the French word "folier" means "to play the fool" and the Italian word "folletto" means a"goblin". The two movable weights E_1 and E_2 attached to the foliot allow one to modify the moment of inertia, and thus the oscillation period of the foliot and the rotatory speed of the wheel.

A vintage drawing of the arrangement is represented in Fig. 9.2. An escapement of this kind is present in the Dover Castle clock built in 1348. It can be seen at the National Museum of Science and Industry, London. In his riveting book [9] C.M. Cipolla agrees with H.A. Lloyd's opinion [10] that "no one knows, and no one probably ever will" who invented such a mechanism but "whatever his name, he was a perfect genius", which explains the enduring interest in these devices [11].

Figure 9.2: Vintage drawing of the verge–and–foliot escapement.

The escapement operation is illustrated in Figs. 9.3 and 9.4. In particular, Fig. 9.3 shows the situation in which the upper blade comes

into contact with one of the teeth of the crown gear and, at the same time, another tooth escapes past the lower blade. From this time instant, the blades and the foliot begin to move clockwise with reference to the drawing. Fig. 9.4 shows the situation in which the lower blade is hit and the foliot begins to move counterclockwise. By denoying with n the odd number of teeth, the angle between two of them (pitch) is $\alpha = 2\pi/n$ so that the situations depicted in Figs. 9.3 and 9.4 are $\alpha/2$ apart.

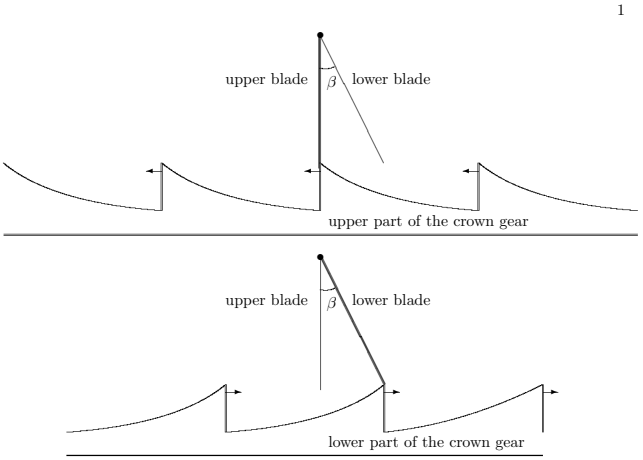

Figure 9.3: Escapement operation: time instant in which the upper blade is hit by a tooth and the lower blade is released.

9.2 Inelastic collisions

To arrive at a simple, yet insightful, model of the system behaviour, in this section it is assumed that the collisions between the blades on the verge and the teeth on the crown gear are wholly inelastic, although in real operation they are not so. Under this hypotesis, the blade and the incident tooth move together after each collision. This tooth keeps on carrying the blade until the latter is released. In order that at the same time the other blade may be engaged by the tooth that reaches the opposite extreme of the vertical diameter of the crown gear, the following condition must be satisfied:

$$r_2 \sin(\beta) = r_1 \sin\left(\frac{\alpha}{2}\right), \tag{9.1}$$

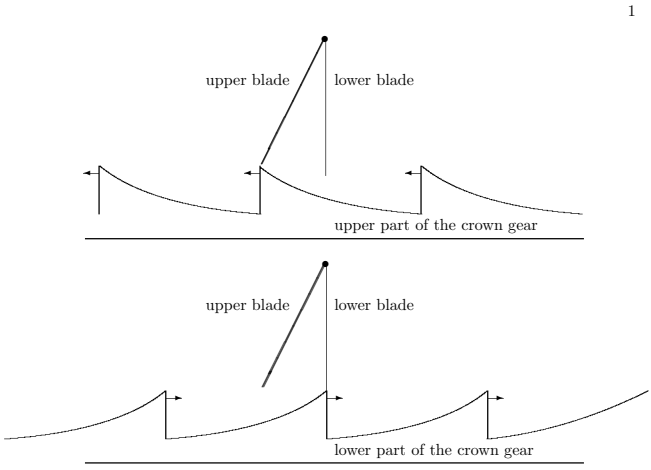

Figure 9.4: Escapement operation: time instant in which the lower blade is hit and the upper blade is released.

where r_1 is the crown radius, r_2 is the common length of the blades (distance of their edges from the axis of the verge), α is the pitch of the gear teeth, and β is the angle of the dihedron formed by the two blades. Otherwise, either the mechanism jams (β too small) or the foliot is not always linked to the crown gear (β too large). Furthermore, all collisions take place at the extremes of the vertical diameter of the crown gear.

If α and β are small, then $\alpha \simeq \sin(\alpha) \simeq \tan(\alpha)$, $\beta \simeq \sin(\beta) \simeq \tan(\beta)$, and the distance from the verge axis of the point of the blade currently in contact with a tooth does not appreciably differ from r_2. In particular, relation (9.1) may be approximated by

$$r_2\beta = r_1\frac{\alpha}{2}. \tag{9.2}$$

By denoting the angular velocities of the crown gear and the foliot by ω_1 and ω_2, respectively, and indicating with the subscripts $-$ and $+$ their velocities immediately before and after each inelastic collision, the angular velocities ω_{1-} and ω_{1+} have the same sign (say positive), and ω_{2-} and ω_{2+} have opposite signs. If $\omega_{2-} > 0$, then

$$r_1\omega_{1-} = r_2\omega_{2-}, \quad r_1\omega_{1+} = -r_2\omega_{2+} \tag{9.3}$$

so that

$$\omega_{1-} = \frac{r_1}{r_2}\omega_{2-}, \quad \omega_{1+} = -\frac{r_1}{r_2}\omega_{2+} \tag{9.4}$$

According to the law of action and reaction, the force exerted by the colliding tooth on the blade is equal and opposite to the force exerted by the blade on the tooth. By indicating with ι the absolute value of the corresponding force impulses acting on each colliding part, and recalling that under the adopted hypotheses on the signs of ω_1 and ω_2 the resulting torque impulses (relative to their respective centres of rotation) are both negative, their values are $-\iota r_1$ and $-\iota r_2$. Equating these torque impulses with the changes of the angular momenta of the crown gear system and of the verge–and–foliot system, respectively, leads to

$$J_1(\omega_{1+} - \omega_{1-}) = -\iota r_1, \quad J_2(\omega_{2+} - \omega_{2-}) = -\iota r_2, \tag{9.5}$$

where J_1 is the crown–gear moment of inertia and J_2 the verge–and–foliot moment of inertia. Due to the very short time of the collision, the other external forces have been neglected.

From (9.4) and (9.5) it follows in particular that

$$\omega_{1+} = \frac{J_1 - \hat{J}_2}{J_1 + \hat{J}_2}\,\omega_{1-} \tag{9.6}$$

and

$$\iota r_1 = 2\frac{J_1 \hat{J}_2}{J_1 + \hat{J}_2}\,\omega_{1-}, \tag{9.7}$$

where

$$\hat{J}_2 = J_2\left(\frac{r_1}{r_2}\right)^2 \tag{9.8}$$

is the moment of inertia of the verge–and–foliot system referred to the crown–gear axis. The same results are obtained by assuming $\omega_{2-} < 0$.

The torque impulses are exerted when the angle ϑ_1 made by the radial edge of a reference tooth with the upward radius of the crown gear is a multiple of $\alpha/2$, that is,

$$\vartheta_1 = k\,\frac{\alpha}{2} \tag{9.9}$$

with k integer. In the interval between two consecutive impulses, under the assumption of linearity, the crown–gear motion is described by

$$T = \big(J_1 + \hat{J}_2\big)\frac{d\omega_1}{dt} + \big(F_1 + \hat{F}_2\big)\omega_1 \tag{9.10}$$

in which T is the torque due to the prime mover (falling weight), F_1 is the friction coefficient of the crown–gear system, and $\hat{F}_2$ is the friction coefficient of the verge–and–foliot system referred to the gear axis.

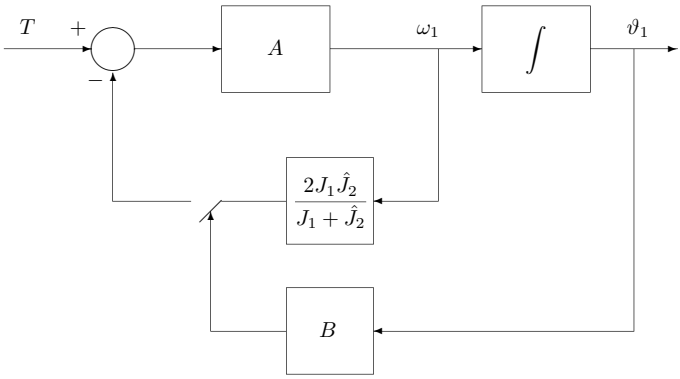

Figure 9.5: Block diagram describing the crown–gear motion under the assumption of inelastic collisions. The sampler is actuated by block B whenever (9.9) is verified. Block A accounts for (9.10); its transfer function is $1/[(J_1 + \hat{J}_2)s + F_1 + \hat{F}_2]$.

9.3 Block diagram and simulation

By taking into account the analysis of Section 9.2, the escapement operation can be represented as in the block diagram of Fig. 9.5, where block A accounts for (9.10). Essentially, the mechanism can be interpreted as a sampled–feedback velocity control system in which the sampling takes place in the feedback path. The amplitude of the torque impulses is proportional to the current angular velocity via the coefficient $2J_1\hat{J}_2/(J_1 + \hat{J}_2)$ according to (9.7).

The time interval between two consecutive impulses is constant at steady state only. Fig. 9.6 shows how the speed of the crown gear varies in time starting from $\vartheta_1(0) = k\alpha/2$ and $\omega_1(0) = 0$, under the assumption that $F_1 = F_2 = 0$ (frictionless bearings): in this case the left–hand block of the forward path in Fig. 9.5 is a pure integrator. Even if this hypotesis is not realistic, it lends itself well to showing that the average speed would indefinitely increase without the escapement mechanism. This result is obviously related to the fact that the change in the potential energy of the weight (the prime mover) is equal to the energy loss in the inelastic collisions.

In the time interval of duration $\Delta t_i = t_i - t_{i-1}$ betwee the $(i-1)$th

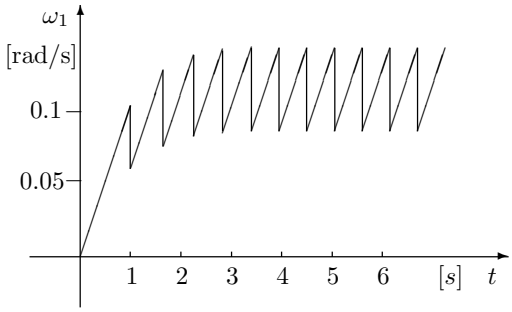

Figure 9.6: Crown–gear angular velocity ω_1 vs. time starting from $\omega_1(0) = 0$ and $\vartheta_1(0) = k\alpha/2$.

collision and the ith collision, the crown gear velocity changes according to

$$\omega_{1,i-} = \omega_{1,i-1+} + \gamma \Delta t_i = \lambda \omega_{1,i-1-} + \gamma \Delta t_i \tag{9.11}$$

and

$$\frac{\alpha}{2} = \frac{\omega_{1,i-1+} + \omega_{1,i-}}{2} \Delta t_i = \frac{\lambda \omega_{1,i-1-} + \omega_{1,i-}}{2} \Delta t_i, \tag{9.12}$$

where, again, subscripts $-$ and $+$ refer to the situations immediately preceding and following the collision,

$$\gamma = \frac{T}{J_1 + \hat{J}_2} \tag{9.13}$$

is the angular acceleration (constant under the considered assumption), and

$$\lambda = \frac{J_1 - \hat{J}_2}{J_1 + \hat{J}_2}. \tag{9.14}$$

From these relations, the following nonlinear recursion is obtained:

$$\omega_{1,i-}^2 = \lambda^2 \omega_{1,i-1-}^2 + \gamma\alpha \tag{9.15}$$

and

$$\Delta t_i = \frac{1}{\gamma} \left[\sqrt{\gamma\alpha + \lambda^2 \omega_{1,i-1-}^2} - \lambda \omega_{1,i-1-} \right]. \tag{9.16}$$

The steady–state angular velocity ω_s at the end of the interval between two consecutive collisions and the corresponding (constant) duration Δt_s

of this interval are

$$\omega_s = \sqrt{\gamma\alpha \frac{J_1^2 + \hat{J}_2^2}{2J_1\hat{J}_2}} \tag{9.17}$$

and

$$\Delta t_s = \sqrt{\frac{\alpha\hat{J}_2}{\gamma J_1}}. \tag{9.18}$$

Fig. 9.6 refers to the following indicative values of the parameters: $\alpha = 2\pi/61 = 0.103$ rad, $\gamma = 0.106\,\mathrm{rad/sec^2}$, $\lambda = 0.6$, which correspond to a rather large speed change at each collision instant. Note that, if F_1 and $\hat{F}_2$ differ from zero, the slanted segments with the same slope in Fig. 9.6 become arcs of exponentials with the same time constant but the behaviour does not change substantially.

9.4 Elastic collisions

If the collisions between the blades and the crown–gear teeth are wholly elastic, that is, without energy losses, the colliding parts are in contact only at the collision instants, whereas in the time interval between consecutive collisions they move separately. In particular, the subsystem formed by the foliot and the verge with its blades moves freely and its velocity is reduced by friction starting from the value acquired when the blade is struck, and the subsystem connected to the crown gear moves under the action of the falling weights. The situation is illustrated in Fig. 9.7 which refers to a time instant following the collision of the tooth a with the lower blade and preceding the collision of the tooth b with the upper blade.

To construct the model of the overall system, it is necessary: (i) to determine the displacement of the tooth edges and the blades, which in turn allows us to determine the collision instants, and (ii) to write down the equations for the angular momenta and the kinetic energies before and after each elastic collision. Unlike the case of inelastic collisions, the model must account for the motion of both subsystems that interact at the collision instants only.

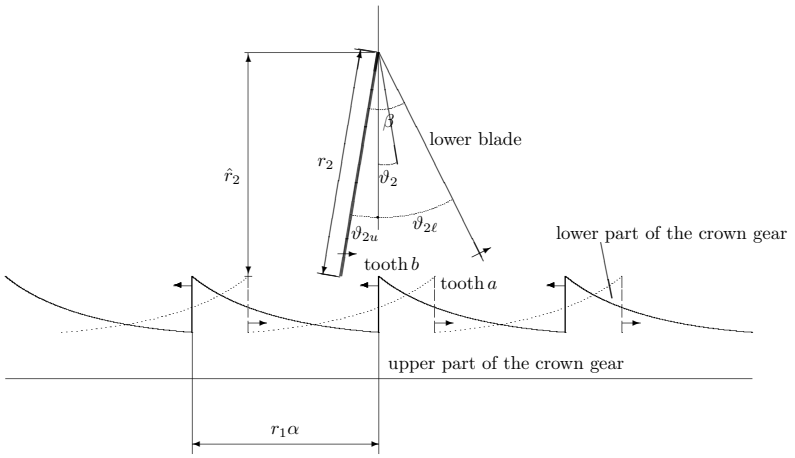

Figure 9.7: Elastic collisions. Top elevation of the escapement mechanism.

Motion equations

The motion of the crown gear (with the other parts joined to it) is described by the equation:

$$T = J_1 \frac{d\omega_1}{dt} + F_1\omega_1 \tag{9.19}$$

and the motion of the verge–and–foliot arrangement by

$$0 = J_2 \frac{d\omega_2}{dt} + F_2\omega_2, \tag{9.20}$$

where the moments of inertia and the friction coefficients are referred to the respective axes of rotation. Obviously, the angle ϑ_1 made by a reference tooth with the vertical axis is the integral of ω_1, and the angular displacement ϑ_2 of the line bisecting the angle between the blades with respect to the vertical line in Fig. 9.7 is the integral of ω_2.

Collisions' angular displacements

The collisions between teeth and blades may reasonably occur within an angle 2α centred at the vertical diameter. Two teeth are included

in this interval both in the upper and in the lower part of the gear and their angular displacements are

$$\vartheta_{1u,a} = \left[\frac{\vartheta_1}{\alpha} - \left\lfloor \frac{\vartheta_1}{\alpha} \right\rfloor\right] \alpha \quad \text{and} \quad \vartheta_{1u,b} = \vartheta_{1u,a} - \alpha \tag{9.21}$$

for the upper teeth, and

$$\vartheta_{1\ell,a} = \left[\frac{\vartheta_1 - \alpha/2}{\alpha} - \left\lfloor \frac{\vartheta_1 - \alpha/2}{\alpha} \right\rfloor\right] \alpha \quad \text{and} \quad \vartheta_{1\ell,b} = \vartheta_{1\ell,a} - \alpha \tag{9.22}$$

for the lower teeth.
Similarly, the angular displacements of the upper and lower blade turn out to be, respectively,

$$\vartheta_{2u} = \begin{cases} \hat{\vartheta}_{2u} := \left[\dfrac{\vartheta_2 + \beta/2}{2\pi} - \left\lfloor \dfrac{\vartheta_2 + \beta/2}{2\pi} \right\rfloor\right] 2\pi & \text{if } \hat{\vartheta}_{2u} \in [0, \pi) \\ \hat{\vartheta}_{2u} - 2\pi & \text{otherwise} \end{cases} \tag{9.23}$$

and

$$\vartheta_{2\ell} = \begin{cases} \hat{\vartheta}_{2\ell} := \left[\dfrac{\vartheta_2 - \beta/2}{2\pi} - \left\lfloor \dfrac{\vartheta_2 - \beta/2}{2\pi} \right\rfloor\right] 2\pi & \text{if } \hat{\vartheta}_{2\ell} \in [0, \pi) \\ \hat{\vartheta}_{2\ell} - 2\pi & \text{otherwise.} \end{cases} \tag{9.24}$$

Using the symbols in Fig. 9.7, the collisions with the upper blade take place when

$$\hat{r}_2 \tan \vartheta_{2u} = r_1 \sin \vartheta_{1u,a} \text{ for } \vartheta_{2u} \geq 0, \text{ or } r_2 \sin \vartheta_{2u} = r_1 \sin \vartheta_{1u,b} \text{ for } \vartheta_{2u} < 0 \tag{9.25}$$

and those with the lower blade when

$$\hat{r}_2 \tan \vartheta_{2\ell} = -r_1 \sin \vartheta_{1\ell,a} \text{ for } \vartheta_{2\ell} < 0, \text{ or } r_2 \sin \vartheta_{2\ell} = -r_1 \sin \vartheta_{1\ell,b} \text{ for } \vartheta_{2\ell} \geq 0. \tag{9.26}$$

By approximating the trigonometric functions by their arguments and $\hat{r}_2$ by r_2, conditions (9.25) and (9.26) become, respectively

$$r_2 \vartheta_{2u} = r_1 \vartheta_{1u,a} \text{ or } r_2 \vartheta_{2u} = r_1 \vartheta_{1u,b} \tag{9.27}$$

and

$$r_2 \vartheta_{2\ell} = -r_1 \vartheta_{1\ell,a} \text{ or } r_2 \vartheta_{2\ell} = -r_1 \vartheta_{1\ell,b}. \tag{9.28}$$

Velocity jumps

Using the symbols of Section 9.4, the equation expressing the energy conservation is

$$J_1\omega_{1-}^2 + J_2\omega_{2-}^2 = J_1\omega_{1+}^2 + J_2\omega_{2+}^2 \ . \tag{9.29}$$

According to Newton's third law of motion applied to the tooth–blade interaction:

$$\frac{J_1\omega_{1+} - J_1\omega_{1-}}{r_1} = -\frac{J_2\omega_{2+} - J_2\omega_{2-}}{r_2} \tag{9.30}$$

so that (retaining only the solution of interest)

$$\omega_{1+} = \frac{J_1 - \hat{J}_2}{J_1 + \hat{J}_2}\,\omega_{1-} + \frac{2\hat{J}_2}{J_1 + \hat{J}_2}\frac{r_2}{r_1}\,\omega_{2-} \ , \tag{9.31}$$

$$\omega_{2+} = \frac{2J_1}{J_1 + \hat{J}_2}\frac{r_1}{r_2}\,\omega_{1-} + \frac{J_1 - \hat{J}_2}{J_1 + \hat{J}_2}\,\omega_{2-} \ . \tag{9.32}$$

Therefore, the magnitude ι of the force impulses as a function of the velocities before the collision is

$$\iota = \frac{2J_1J_2}{J_1r_2^2 + J_2r_1^2}\,[|r_2\omega_{2-}| + |r_1\omega_{1-}|] \tag{9.33}$$

both for the collision with the upper blade and for that with the lower one.

With the adopted sign convention, the feedback torque impulse acting on the crown gear is

$$\Delta T_1 = -\,r_1\,\iota \tag{9.34}$$

and that acting on the blade is

$$\Delta T_2 = \pm\,r_2\,\iota, \tag{9.35}$$

where the sign + applies to the collision with the upper blade and the sign − to the one with the lower blade.

Block diagram

All of the previous relations are represented by the block diagram in Fig. 9.8. The left part of the block diagram refers to the crown–gear system and the right part to the verge–and–foliot system. The upper part refers to the collisions with the upper blade and the lower part to those with the lower blade. Blocks 1 and 2 account, respectively, for (9.19) and (9.20). Blocks 3 and 4 are pure integrators. Blocks 5 and 6 correspond to (9.21) and (9.22): they allow us to compute the angular displacement of the tooth of interest from the displacement ϑ_1 of an arbitrary reference tooth. Similarly, blocks 7 and 8 supply the displacements of each blade from ϑ_2 according to (9.23) and (9.24). Blocks 9 and 10 actuate the samplers when conditions (9.27) or, respectively, (9.28) are satisfied. The outputs of the samplers are force impulses whose amplitudes are given by blocks 11 and 12 according to (9.33). By multiplying such force impulses by their respective radii, the feedback torque impulses (9.34) and (9.35) are obtained.

9.5 Concluding remarks

The verge–and–foliot escapement of medieval mechanical clocks represents an important contribution of automatic control technology. The operation of this accurate velocity regulator is based on feedback even if, quite likely, the unknown inventor of this ingenious contrivance was not aware of the feedback nature of the control system he had conceived and, in fact, Otto Mayr [3] does not consider the verge–and–foliot clock as an example of closed–loop control.

The motion of the escapement has been analyzed in the cases of both inelastic and elastic collisions between its component parts. The block diagrams describing the verge–and–foliot operation have been derived. Simulations show that the average steady–state gear velocity, directly related to the movement of the clock hand, remains constant.

1

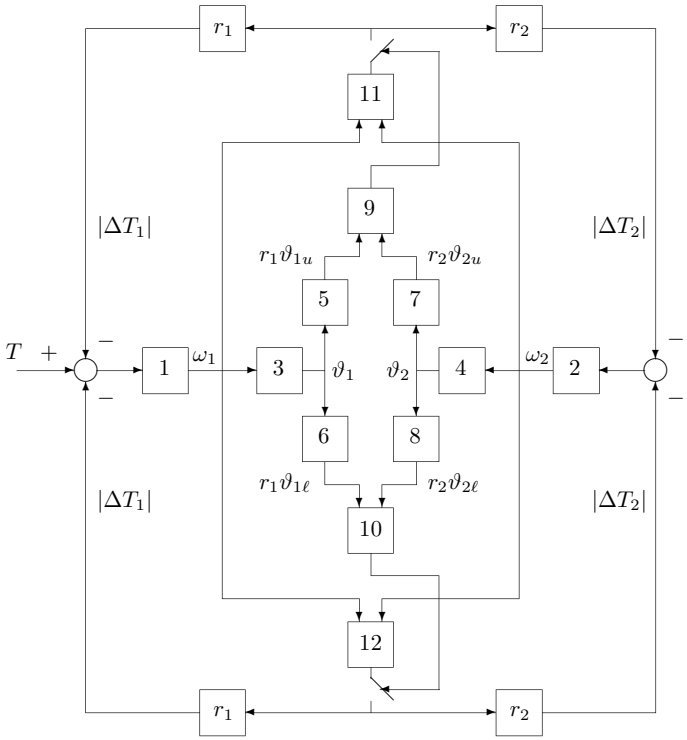

Figure 9.8: Block diagram describing the operation of the verge–and–foliot escapement under the assumption of elastic collisions between crown–gear teeth and blades.

Bibliography

[1] A. Lepschy and U. Viaro, "Feedback: a technique and a *tool for thought*", in M. Lucertini, A. Millán Gasca, and F. Nicolò, Eds., *Technological Concepts and Mathematical Models in the Evolution of Modern Engineering Systems*, Birkhäuser, Basel, pp. 129–155, 2004.

[2] H. Diels, *Antike Technik*, Teubner, Berlin, 1920 (2nd edition).

[3] O. Mayr, *The Origins of Feedback Control*, The M.I.T. Press, Cambridge, MA, 1970.

[4] D.S. Bernstein, "Feedback control: an invisible thread in the history of technology", IEEE Control Syst. Mag., vol. 22, no. 2, pp. 53–68, 2002.

[5] A. Lepschy, G.A. Mian, and U. Viaro, "Feedback control in ancient water and mechanical clocks", IEEE Trans. Education, vol. 35, no. 1, pp. 3–10, 1992.

[6] D. Alighieri, *Commedia*, Garzanti, Milano, 1987 (Paradiso, X, 139–144; XXIV, 13–14). English translation by C.E. Norton, *The Divine Comedy of Dante Alighieri*, W. Benton - Encyclopaedia Britannica, Chicago, 1952.

[7] A.V. Roup, D.S. Bernstein, S.G. Neresov, W.M. Haddad, and V. Chellaboina, "Limit cycle analysis of the verge and foliot clock escapament using impulsive differential equations and Poincaré maps", Int. J. Control, vol. 76, no. 17, pp. 1685–1698, 2003.

[8] T.K. Derry and T.I. Williams, *A Short History of Technology*, Clarendon, Oxford, 1960.

[9] C.M. Cipolla, *Clocks and Culture 1300–1700*, Collins, London, 1967.

[10] H.A. Lloyd, *Some Outstanding Clocks over Seven Hundred Years 1250–1950*, Leonard Hill, London, 1958.

[11] B. Danese and S. Oss, "A medieval clock made out of simple materials", Eur. J. Phys., vol. 29, no. 4, pp. 799–814, 2008.

Often, short papers tend to be sharper than longer works because they focus on a single theme without lingering on unessential aspects, thus showing clearly the signicance of a contribution or an idea. The author of this book had the privilege of collaborating for over a quarter of a century with Antonio Lepschy (1931-2005), a recognized leader of the Italian control community.

Lepschy had a liking for the brief paper format, so that many results obtained by his research team were published in this way. The present compilation tells a few of these short stories, duly updated, trying to preserve their original flavour.

Umberto Viaro (http://umbertoviaro.blogspot.com/) has been professor of System and Control Theory at the University of Udine, Italy, since 1994. His 25-year-long collaboration with Antonio Lepschy resulted in more than 100 joint papers and two books. An essential role in this research activity was played by Wiesław Krajewski of the Systems Research Institute, Polish Academy of Sciences. The current research interests of Umberto Viaro concern optimal model reduction, robust control, switching and LPV control. He is the author or coauthor of 4 books and about 180 research papers.

ISSN 0208-8029
ISBN 9788389475282

SYSTEMS RESEARCH INSTITUTE
POLISH ACADEMY OF SCIENCES
Phone: (+48) 22 3810246 / 22 3810241 / 22 3810273
tel. (22) 3810 277; e-mail: biblioteka@ibspan.waw.pl